JOURNAL OF GUIDANCE, CONTROL, AND DYNAMICS
Vol. 24, No. 1, January–February 2001

Analysis of Longitudinal Flight Dynamics: A Bifurcation-Theoretic Approach

Der-Cherng Liaw* and Chau-Chung Song†
National Chiao Tung University, Hsinchu 30010, Taiwan, Republic of China

Bifurcation theory has been used to study the nonlinear dynamics and stability of many modern aircraft, especially in broad angle-of-attack flight dynamics. However, the main application of bifurcation analysis is based on numerical simulations to predict and explain the nonlinear instability of flight dynamics by the use of parametric continuation methods. Bifurcation theory is applied to theoretically analyze the nonlinear phenomena of longitudinal flight dynamics, by the choice of the elevator deflection and mass of the aircraft as system parameters. Both stationary and Hopf bifurcations may appear at some critical values of elevator command. Discontinuity also may occur at system equilibria as system parameters vary. The bifurcation phenomena occurring in nonlinear aircraft dynamics might result in jump behaviors, pitch oscillations, or system instabilities. Numerical study of a simple third-order model of longitudinal dynamics verifies the theoretical analysis. Qualitative results are obtained to understand the longitudinal flight dynamics.

Nomenclature

C_{L_w}, C_{L_t}	=	coefficients of wing and tail lift forces, respectively
$C^i_{L_w}$, $C^i_{L_t}$	=	coefficients of approximated wing and tail lift forces, respectively
$c\dot{\theta}$	=	damping moment
$f^{(n,0)}(x, y)$	=	nth partial derivative of function f with respect to x
$f^{(0,n)}(x, y)$	=	nth partial derivative of function f with respect to y
$f'(x)$	=	derivative of function f with respect to x
g	=	gravitation constant
I_x, I_y, I_z	=	moments of inertia about axes x, y, and z, respectively
L_w, L_t	=	wing and tail lift forces, respectively
l	=	distance between wing aerodynamic center (a.c.) and aircraft's center of gravity
l_t	=	distance between tail a.c. and aircraft's center of gravity
M_w	=	wing pitching moment
m	=	mass of aircraft
p, q, r	=	roll, pitch, and yaw rates, respectively
$\bar{q}$	=	dynamic pressure
S, S_t	=	wing and horizontal tail area, respectively
u, v, w	=	velocity components along x, y, and z axes, respectively
α, α_t	=	wing and tail angle of attack, respectively
δ_e	=	elevator deflection angle
θ	=	pitch angle

I. Introduction

MODERN high-performance fighter aircraft are being designed for maneuvers at ever-increasing angle of attack. However, high-angle-of-attack flight, although offering a substantial increase in agility, implies a greater risk of loss of flight stability. It is known that aircraft, during high-angle-of-attack maneuvers, may undergo abrupt and nonlinear transitions. These phenomena include a jump between two rival equilibrium states and transitions from system equilibrium to periodic motion (or the so-called limit cycle) as the control parameter varies.

Received 27 April 1999; revision received 20 April 2000; accepted for publication 21 April 2000.

*Associate Professor, Department of Electrical and Control Engineering; dcliaw@cc.nctu.edu.tw.

†Ph.D. Student, Department of Electrical and Control Engineering.

Recently, the study of the nonlinear phenomena occurring in flight dynamics has attracted much attention.[1–6] Most of these studies tried to find the linkage between bifurcation phenomena and the nonlinear motion of flight dynamics such as oscillations, jump behavior, and stall. For instance, both stationary and Hopf bifurcations were observed for several aircraft models.[1–3] Bifurcation analysis of a highly augmented aircraft model of an F-16 fighter was presented in Ref. 4. The effect of control efforts on the flight dynamics was studied using bifurcation techniques and a simple nonlinear aircraft model.[5] Jahnke and Culick[6] studied the nonlinear dynamics of the F-14 fighter. Both stationary and Hopf bifurcations were observed and used to predict the onset of system instabilities such as jump phenomena. A major advantage of a bifurcation study of flight dynamics is to provide more understanding and prediction of possible nonlinear behaviors and corresponding characteristics. Though bifurcation phenomena have been observed to link with nonlinear motions in flight dynamics, most of the existing studies were obtained by numerical analysis.

In recent years, bifurcation theory and corresponding analysis techniques[7–11] have been well exploited. These methods have been successfully applied to the study and control of longitudinal flight dynamics,[12,13] stabilization of tether satellite systems[14] and jet engine compressors.[15] In Refs. 12 and 13, the stabilization issue of a given trim condition of an aircraft arbitrarily close to the stall angle was studied for the F-8 Crusader. Based on the so-called pseudo-steady-state approach, a reduced second-order model is abstracted from the one proposed in Ref. 16 for the design of a controller. From a bifurcation theorem, a warning signal, which is prompted by a small-amplitude, stable limit-cycle-type pitching motion of the aircraft, was proposed to get the attention of the pilot in the case of impending stall.

Instead of using a numerical approach, the main goal of this paper is to provide an analytical study of longitudinal flight dynamics. Based on previous successful applications of bifurcation theory to the analytic study of a tether satellite system[14] and a jet engine compressor[15] by Liaw and Abed, the existence and stability conditions of system equilibria and local bifurcations in pitch axis flight dynamics will be analytically studied. The linkage between theoretical analysis and numerical simulation of bifurcation phenomena will be constructed. In addition, the relationship between the nonlinear behavior of aircraft dynamics and the bifurcation phenomena arising from the nonlinear model of flight dynamics will also be investigated. To have better understanding of nonlinear behavior in longitudinal motion, the study of the second-order reduced model[12,13] will be extended to the third-order pitch axis flight dynamics. Numerical analysis will be devoted to the longitudinal dynamics for an F-8 aircraft and the relationship between

the findings of this study and existing observations will also be discussed.

The organization of this paper is as follows. In Sec. II, we recall some basic concepts of bifurcation theory and establish the model of the pitch axis flight dynamics that will be used throughout the paper. This is followed by the dynamic analysis of local stability and bifurcation phenomena of the third-order flight dynamic model. In addition to the derivation of stability conditions for system equilibria, in Sec. III we will also study the possibility of the occurrence of local bifurcations and the corresponding stability. Numerical studies of the dynamic behavior of F-8 aircraft will be given to verify the theoretical results attained in Sec. III. Finally, concluding remarks are given in Sec. V.

II. Setup

A. Simple Bifurcations

In this section, we recall some of theoretical results[7–11] of the occurrence of bifurcations of one-parameter families of nonlinear systems. With these, a stability equivalence of one special system is presented, which will be applied in the next section to study the dynamic behavior of longitudinal flight systems.

Consider one-parameter families of nonlinear ordinary differential equations as given by

$$\dot{\boldsymbol{x}} = \boldsymbol{f}(\boldsymbol{x}, \mu) \tag{1}$$

where $\boldsymbol{x} \in \mathbb{R}^n$, $\mu \in \mathbb{R}$, and $\boldsymbol{f}$ is a smooth function. The equilibrium solutions of Eq. (1), which are given by the solutions of the equation $\boldsymbol{f}(\boldsymbol{x}, \mu) = 0$, clearly depend on μ. As μ varies, the implicit function theorem implies that these equilibria are given by smooth functions of μ. Each such equilibrium path is called a branch of equilibria of Eq. (1). Suppose there is a parameter value μ_c and equilibrium $\boldsymbol{x}(\mu_c) = \boldsymbol{x}_0$ at which the Jacobian matrix $D_x \boldsymbol{f}(\boldsymbol{x}_0, \mu_c) \in \mathbb{R}^{n \times n}$ has a zero eigenvalue. The implicit function theorem fails to imply uniqueness, and several branches may join at $\boldsymbol{x}_0$. If such a joining of equilibria occurs, $(\boldsymbol{x}_0, \mu_c)$ is called a point of bifurcation, or a so-called bifurcation point. Specifically, $(\boldsymbol{x}_0, \mu_c)$ is a point at which a stationary (or static) bifurcation occurs. A graph of the solutions $\boldsymbol{x}(\mu)$ vs the bifurcation parameter μ drawn near the bifurcation point $(\boldsymbol{x}_0, \mu_c)$ is called a bifurcation diagram. The nominal system equilibrium is called the trivial solution and the nontrivial solution $\boldsymbol{x}(\mu)$ is called the bifurcated solution.

In the following, for simplicity, we assume that (0, 0) is a bifurcation point of interest, and $\mu_c = 0$ is referred to as the bifurcation value or critical parameter value. In addition, we assume $\boldsymbol{f}(0, \mu) = 0$ for all values of μ. That is, $\boldsymbol{x} = 0$ is a trivial solution of Eq. (1). One of the generic bifurcations that can occur in Eq. (1) is when the Jacobian matrix $D_x \boldsymbol{f}(0, 0)$ possesses a simple zero eigenvalue. Another generic bifurcation specifically discussed in this study is the one at which $D_x \boldsymbol{f}(0, 0)$ has a pair of simple, purely imaginary eigenvalues $\pm i\omega_c$, and no other purely imaginary eigenvalues. Such a phenomenon corresponds to the Hopf bifurcation. Because in linear theory the existence of such purely imaginary eigenvalues implies the existence of periodic solutions of Eq. (1), in some sense Hopf bifurcation always answers the question of whether a periodic solution exists when nonlinearity is accounted for.

We assume that the governing equation of the problem is sufficiently smooth. Therefore, we may assume that Eq. (1) possesses a Taylor series expansion with respect to both the state variable $\boldsymbol{x}$ and the bifurcation parameter μ at the bifurcation point (0, 0) and is given by

$$\dot{\boldsymbol{x}} = \boldsymbol{L}_0 x + \gamma\mu + \boldsymbol{Q}_0(\boldsymbol{x}, \boldsymbol{x}) + \boldsymbol{C}_0(\boldsymbol{x}, \boldsymbol{x}, \boldsymbol{x}) + \cdots + \mu[\boldsymbol{L}_1 \boldsymbol{x} + \boldsymbol{Q}_1(\boldsymbol{x}, \boldsymbol{x}) + \cdots] + \mu^2(\boldsymbol{L}_2 \boldsymbol{x} + \cdots) + \cdots \tag{2}$$

where $\boldsymbol{Q}_k(\boldsymbol{x}, \boldsymbol{x}) := (1/2!k!) D_{\mu^k xx} \boldsymbol{f}(\boldsymbol{x}, \mu)$, $\boldsymbol{C}_k(\boldsymbol{x}, \boldsymbol{x}, \boldsymbol{x}) := (1/3!k!) D_{\mu^k xxx} \boldsymbol{f}(\boldsymbol{x}, \mu)$, and so forth, are the bilinear, trilinear, and so forth, parts of $\boldsymbol{f}(\boldsymbol{x}, \mu)$, respectively, such that $\boldsymbol{Q}_k(\boldsymbol{x}, \boldsymbol{y}) = \boldsymbol{Q}_k(\boldsymbol{y}, \boldsymbol{x})$ and similarly for $\boldsymbol{C}_k(\boldsymbol{x}, \boldsymbol{y}, \boldsymbol{z})$, and so forth. Obviously, $\boldsymbol{L}_0$ corresponds to the Jacobian $D_x \boldsymbol{f}(0, 0)$, $\boldsymbol{L}_k := (1/k!) D_{\mu^k x} \boldsymbol{f}(0, 0)$ and $\gamma = D_\mu \boldsymbol{f}(0, 0)$. Note that if the system (1) has the origin as an equilibrium point for all μ in a neighborhood of (0, 0), then $\gamma = 0$ in Eq. (2).

Denote $\boldsymbol{L}(\mu) := \boldsymbol{L}_0 + \mu\boldsymbol{L}_1 + \mu^2\boldsymbol{L}_2 + \cdots$ the overall Jacobian matrix of Eq. (2). Thus, it is clear that the eigenvalue $\lambda(\mu)$ that emerges from the critical mode depends on the value of μ. Furthermore, as μ varies over the critical value 0, the real part of $\lambda(\mu)$ may change from being positive to being negative or vice versa. This is often known as crossing.

Denote $\boldsymbol{l}$ and $\boldsymbol{r}$ the left and right eigenvectors associated with the eigenvalue $\lambda(\mu)$, respectively, and suppose that $\lambda(0) = 0$. Because $\boldsymbol{L}(\mu)\boldsymbol{r}(\mu) = \lambda(\mu)\boldsymbol{r}(\mu)$, we have

$$\frac{\mathrm{d}}{\mathrm{d}\mu}[\boldsymbol{L}(\mu)\boldsymbol{r}(\mu)] = \frac{\mathrm{d}}{\mathrm{d}\mu}[\lambda(\mu)\boldsymbol{r}(\mu)]$$

Therefore,

$$\boldsymbol{l}[\boldsymbol{L}'(\mu)\boldsymbol{r}(\mu) + \boldsymbol{L}(\mu)\boldsymbol{r}'(\mu)]|_{\mu=0} = \boldsymbol{l}[\lambda'(\mu)\boldsymbol{r}(\mu) + \lambda(\mu)\boldsymbol{r}'(\mu)]|_{\mu=0}$$

implying that

$$\lambda'(0) = \boldsymbol{l}\boldsymbol{L}_1\boldsymbol{r}$$

where $\boldsymbol{L}_1$ is as in Eq. (2) and we choose $\boldsymbol{l} \cdot \boldsymbol{r} = 1$. The transversality condition for stationary bifurcation is

$$\lambda'(0) = \boldsymbol{l}\boldsymbol{L}_1\boldsymbol{r} \neq 0 \tag{3}$$

Especially for saddle-node bifurcation, Eq. (3) is equivalent to

$$\boldsymbol{l}\gamma \neq 0 \tag{4a}$$

and

$$\boldsymbol{l}\boldsymbol{Q}_0(\boldsymbol{r}, \boldsymbol{r}) \neq 0 \tag{4b}$$

For Hopf bifurcation, this is modified to be

$$\Re e(\boldsymbol{l}\boldsymbol{L}_1\boldsymbol{r}) \neq 0 \tag{5}$$

The transversality condition implies that the eigenvalue $\lambda(\mu)$ with $\Re e[\lambda(0)] = 0$ strictly crosses the imaginary axis and with a nonzero speed.

B. Mathematical Model of Longitudinal Flight Dynamics

In the following, we recall the model of longitudinal flight dynamics from Ref. 16 and establish the mathematical models that will be employed in this paper.

Consider the coordinate system for longitudinal flight dynamics as depicted in Ref. 16. Suppose that the aerodrag is small compared with the lift force and the weight of the airplane, and that it is neglected in the analysis. The basic equations of motion for longitudinal dynamics with drag and thrust neglected are given as

$$m(\dot{u} + w\dot{\theta}) = -mg\sin\theta + L_w \sin\alpha + L_t \sin\alpha_t \tag{6a}$$

$$m(\dot{w} - u\dot{\theta}) = mg\cos\theta - L_w \cos\alpha - L_t \cos\alpha_t \tag{6b}$$

$$I_y\ddot{\theta} = M_w + lL_w \cos\alpha - l_t L_t \cos\alpha_t - c\dot{\theta} \tag{6c}$$

Suppose the tail and wing lift forces are given by $L_w = C_{L_w}\bar{q}S$ and $L_t = C_{L_t}\bar{q}S_t$, respectively. By using $w = u\tan\alpha$ and $\dot{w} = \dot{u}\tan\alpha + u\dot{\alpha}\sec^2\alpha$, we can rewrite Eq. (6) as

$$\dot{u} = -u\dot{\theta}\tan\alpha - g\sin\theta + (L_w/m)\sin\alpha + (L_t/m)\sin\alpha_t \tag{7a}$$

$$\dot{\alpha} = \dot{\theta}\sin^2\alpha + (g/u)\sin\theta\sin\alpha\cos\alpha s - L_w/(um)\sin^2\alpha\cos\alpha - L_t/(um)\sin\alpha\cos\alpha\sin\alpha_t + \dot{\theta}\cos^2\alpha + (g/u)\cos^2\alpha\cos\theta - L_w/(um)\cos^3\alpha - L_t/(um)\cos^2\alpha\cos\alpha_t \tag{7b}$$

$$\ddot{\theta} = M_w/I_y + (lL_w/I_y)\cos\alpha - (l_t L_t/I_y)\cos\alpha_t - (c/I_y)\dot{\theta} \tag{7c}$$

The system as in Eq. (7) represents the fourth-order model of longitudinal flight dynamics of which states are $(u, \alpha, \theta, \dot{\theta})$.

Assume that the aircraft flies at a constant velocity. That is, $\dot{u} = 0$. System (7) can then be reduced to a third-order model

$$\dot{\alpha} = q\cos^2\alpha + (g/u)\cos^2\alpha\cos\theta - L_w/(um)\cos^3\alpha - L_t/(um)\cos^2\alpha\cos\alpha_t \tag{8a}$$

$$\dot{\theta} = q \tag{8b}$$

$$\dot{q} = M_w/I_y + (lL_w/I_y)\cos\alpha - (l_tL_t/I_y)\cos\alpha_t - (c/I_y)q \tag{8c}$$

In the next two sections, we will focus on the study of longitudinal flight dynamics presented in Eq. (8) above.

III. Stability and Bifurcation Analysis

In this section, we derive the stability conditions of the longitudinal flight dynamics. Based on the third-order model of longitudinal dynamics as in Eq. (8), we analyze the stability and bifurcation phenomena for the flight dynamics.

A. Local Stability Analysis

Here, we assume that the wing lift force L_w is a function of the angle of attack α, the tail lift force L_t is a function of both α and the elevator deflection angle δ_e, the wing pitching moment M_w is a function of α, and the tail angle of attack α_t is a function of both α and δ_e, respectively. These are $L_w := L_w(\alpha)$, $L_t := L_t(\alpha, \delta_e)$, $M_w := M_w(\alpha)$, and $\alpha_t := \alpha_t(\alpha, \delta_e)$.

We can then rewrite Eq. (8) as follows:

$$\dot{\alpha} = q\cos^2\alpha + (g/u)\cos^2\alpha\cos\theta - L_w(\alpha)/(um)\cos^3\alpha - L_t(\alpha, \delta_e)/(um)\cos^2\alpha\cos\alpha_t(\alpha, \delta_e) \tag{9a}$$

$$\dot{\theta} = q \tag{9b}$$

$$\dot{q} = M_w(\alpha)/I_y + [lL_w(\alpha)/I_y]\cos\alpha - [l_tL_t(\alpha, \delta_e)/I_y] \times \cos\alpha_t(\alpha, \delta_e) - (c/I_y)q \tag{9c}$$

Now, we derive the local stability and bifurcation conditions for Eq. (9). Denote $\boldsymbol{x}^0 = [\alpha^0, \theta^0, q^0]^T$ an equilibrium point of the third-order system (9) at a given value of δ_e, for example, $\delta_e = \delta_e^0$. According to the definition of an equilibrium point, we have $q^0 = 0$ and the following two conditions must hold:

$$-L_w(\alpha^0)\cos\alpha^0 + mg\cos\theta^0 - L_t\left(\alpha^0, \delta_e^0\right)\cos\alpha_t\left(\alpha^0, \delta_e^0\right) = 0 \tag{10a}$$

or

$$\cos^2\alpha^0 = 0 \tag{10b}$$

$$M_w(\alpha^0) + lL_w(\alpha^0)\cos\alpha^0 - l_tL_t\left(\alpha^0, \delta_e^0\right)\cos\alpha_t\left(\alpha^0, \delta_e^0\right) = 0 \tag{10c}$$

First, consider the case of $\cos^2\alpha^0 = 0$. Then we have $\alpha^0 = n\pi + (\pi/2)$ for $n = 0, 1, 2, 3, \ldots$.

Because an aircraft can not easily maintain such a high-angle-of-attack flight, in the remainder of this paper we only consider the case of which (10a) holds. Referring to Eq. (10c), we can rewrite Eq. (10a) as

$$M_w(\alpha^0) + (l + l_t)L_w(\alpha^0)\cos\alpha^0 = l_tmg\cos\theta^0 \tag{11}$$

It is clear that Eqs. (10c) and (11) represent the relationship among α^0, δ_e^0, and θ^0. We can obtain the solution of α^0 from Eq. (10c) for given δ_e^0, whereas Eq. (11) provides the solution of θ^0. However, the solutions of α^0 and θ^0 from Eqs. (10c) and (11) may not exist. We have the following two observations from Eqs. (10c) and (11).

Observation 1: In general, $M_w(\alpha^0)$ is a nonnegative value. Then Eq. (11) has no solution for some values of θ^0 if $(l + l_t)L_w(\alpha^0) > l_tmg$.

Observation 2: Because a cosine function is an even function, $-\theta^0$ is also a solution of Eq. (11) if θ^0 is a solution of Eq. (11) for a given value of α^0.

From Observations 1 and 2, the number of equilibrium points of Eq. (9) may be zero, one, or two for given $\delta_e = \delta_e^0$ in a fixed interval of θ^0, the extent of which is 2π. Specifically, system (9) has only one equilibrium point at $\theta^0 = 0$ in the interval $\theta^0 \in (-\pi, \pi)$ if it exists. We then have the next result.

Proposition 1: System (9) may have saddle-node bifurcation at $x^0 = [\alpha^0, 0, 0]^T$ if $\boldsymbol{x}^0$ is an equilibrium point of system (9).

Note that, it is not difficult to find from Observation 1 that the aircraft's mass m also plays a key role in determining the existence of the system equilibria of system (9). That is, there is no equilibrium point of system (9) for given $\delta_e = \delta_e^0$ if $m < 1/(l_tg)\{(l + l_t)L_w(\alpha^0)\}$.

According to Observations 1 and 2, it is known that, although the saddle-node bifurcation happens at system (9), the system equilibria disappear in a fixed interval of parameter variation. This implies that the aircraft dynamics might suddenly undergo a jump transition such as stall behavior.

Next, we will derive the stability conditions for an equilibrium point $\boldsymbol{x}^0$ of system (9). For given state $[\alpha, \theta, q]^T$ of system (9), denote $\boldsymbol{x} = [x_1, x_2, x_3]^T$ the state variation of $\boldsymbol{x}$ near the equilibrium point $\boldsymbol{x}^0$, where $x_1 = \alpha - \alpha^0$, $x_2 = \theta - \theta^0$, and $x_3 = q$. Also, let $u_\delta = \delta_e - \delta_e^0$ denote the control input.

The linearization of the system (9) at $\boldsymbol{x}^0$ and $\delta_e = \delta_e^0$ gives

$$\dot{\boldsymbol{x}} = \boldsymbol{A}_0\boldsymbol{x} + \gamma u_\delta \tag{12}$$

where

$$\boldsymbol{A}_0 = \begin{bmatrix} a_{11} & a_{12} & a_{13} \\ 0 & 0 & 1 \\ a_{31} & 0 & a_{33} \end{bmatrix} \qquad \gamma = \begin{bmatrix} \gamma_1 \\ 0 \\ \gamma_3 \end{bmatrix}$$

Here, the values of a_{ij} and γ_i are given in Appendix A. We then have the characteristic equation for the linearized model (12) as given by

$$\lambda^3 - (a_{11} + a_{33})\lambda^2 + (a_{11}a_{33} - a_{13}a_{31})\lambda - (a_{12}a_{31}) = 0 \tag{13}$$

By applying the Routh–Hurwitz stability criteria to the linearized model (12) with $u_\delta = 0$, we have the following result.

Proposition 2: The equilibrium point $[\alpha^0, \theta^0, 0]^T$ of system (9) is asymptotically stable if the following three conditions hold.

$$-(a_{11} + a_{33}) > 0 \qquad (\text{or} \quad a_{11} < -a_{33} = c/I_y) \tag{14a}$$

$$-(a_{11} + a_{33})(a_{11}a_{33} - a_{13}a_{31}) + a_{12}a_{31} > 0 \tag{14b}$$

$$-a_{12}a_{31} > 0 \qquad (\text{or} \quad a_{31}\sin\theta^0 > 0) \tag{14c}$$

From Eq. (14c), it is clear that the stability of the equilibrium point $[\alpha^0, \theta^0, 0]^T$ of system (9) strongly depends on the sign of θ^0 in the interval $(-\pi, \pi)$. Under the assumption that both Eqs. (14a) and (14b) hold, we have the following corollary.

Corollary 1: Suppose $\boldsymbol{x}^0 = [\alpha^0, \theta^0, 0]^T$ is an equilibrium point of the system (9) for $\theta^0 \in (-\pi, \pi)$ and both Eqs. (14a) and (14b) hold. Then $\boldsymbol{x}^0$ is asymptotically stable (respectively unstable) for $\theta^0 > 0$ and unstable (respectively stable) for $\theta^0 < 0$ if $a_{31} > 0$ (respectively if $a_{31} < 0$).

B. Local Bifurcation Analysis

In the following, we will study the possible appearance of local bifurcations by treating the elevator command δ_e as a bifurcation parameter. First, taking the Taylor series expansion for the system (9) at $\boldsymbol{x}^0$, we obtain that $\boldsymbol{L}_0 = \boldsymbol{A}_0$,

$$\boldsymbol{Q}_0(\boldsymbol{x}, \boldsymbol{x}) = \begin{bmatrix} q_{11}x_1^2 + q_{12}x_2^2 + q_{13}x_1x_2 + q_{14}x_1x_3 \\ 0 \\ q_{31}x_1^2 \end{bmatrix} \tag{15}$$

and

$$\boldsymbol{C}_0(\boldsymbol{x}, \boldsymbol{x}, \boldsymbol{x}) = \begin{bmatrix} c_{11}x_1^3 + c_{12}x_2^3 + c_{13}x_1^2x_2 + c_{14}x_1x_2^2 + c_{15}x_1^2x_3 \\ 0 \\ c_{31}x_1^3 \end{bmatrix} \tag{16}$$

Here, L_0 denotes the Jacobian matrix, Q_0 and C_0 denote the quadratic and cubic terms, respectively, and the states x_1, x_2, and x_3 are as defined earlier. The values of a_{ij} and q_{ij} are given in Appendices A and B, and the values of c_{ij} are omitted because they are quite complicated. For simplicity, we have the following three definitions:

$$A_w(\alpha^0) = \frac{\mathrm{d}}{\mathrm{d}\alpha}\{L_w(\alpha)\cos\alpha\}\Big|_{\alpha=\alpha^0}$$
$$= L_w'(\alpha^0)\cos\alpha^0 - L_w(\alpha^0)\sin\alpha^0$$

$$A_t(\alpha^0, \delta_e^0) = \frac{\partial}{\partial\alpha}\{L_t(\alpha, \delta_e)\cos\alpha_t(\alpha, \delta_e)\}\Big|_{(\alpha,\delta_e)=(\alpha^0,\delta_e^0)}$$
$$= L_t^{(1,0)}(\alpha^0, \delta_e^0)\cos\alpha_t(\alpha^0, \delta_e^0)$$
$$- L_t(\alpha^0, \delta_e^0)\sin\alpha_t(\alpha^0, \delta_e^0)\alpha_t^{(1,0)}(\alpha^0, \delta_e^0)$$

$$B_t(\alpha^0, \delta_e^0) = \frac{\partial}{\partial\delta_e}\{L_t(\alpha, \delta_e)\cos\alpha_t(\alpha, \delta_e)\}\Big|_{(\alpha,\delta_e)=(\alpha^0,\delta_e^0)}$$
$$= L_t^{(0,1)}(\alpha^0, \delta_e^0)\cos\alpha_t(\alpha^0, \delta_e^0)$$
$$- L_t(\alpha^0, \delta_e^0)\sin\alpha_t(\alpha^0, \delta_e^0)\alpha_t^{(0,1)}(\alpha^0, \delta_e^0)$$

where $A_w(\cdot)$ and $A_t(\cdot,\cdot)$ represent the slopes of lift forces of the wing and tail, which are multiplied by the functions $\cos\alpha$ and $\cos\alpha_t$ with respect to α, respectively, and $B_t(\cdot,\cdot)$ is the slope of tail lift force multiplied by the function $\cos\alpha_t$ with respect to the parameter δ_e.

From the characteristic equation as in Eq. (13), the system (9) has at least one zero eigenvalue if $a_{12}a_{31}=0$. By checking the values of a_{12} and a_{31} (see Appendix A), we have, as a necessary condition for the existence of a zero eigenvalue of system (9), that $\theta^0=0$ because $a_{12}=0$ if $\theta^0=0$.

From Corollary 1, as θ^0 varies near the critical value 0, one eigenvalue of system (12) changes from being positive to negative or vice versa. This implies that the transversality condition holds if $[\alpha^0, 0, 0]^T$ is an equilibrium point of system (9). We then have the next result from Proposition 1.

Lemma 1: Suppose $[\alpha^0, 0, 0]^T$ is an equilibrium point of system (9). Then the system (9) undergoes a saddle-node bifurcation at the critical point $[\alpha^0, 0, 0]^T$ if both Eqs. (14a) and (14b) hold.

To meet the transversality condition as in Eq. (4), the equilibrium point $[\alpha^0, 0, 0]^T$ must satisfy the following two equations:

$$\gamma_1 a_{31} - \gamma_3 a_{11} = -\cos^2\alpha^0 \,|\, (umI_y)\big[M_w'(\alpha^0) + (l + l_t)A_w(\alpha^0, \delta_e^0)\big]B_t(\alpha^0, \delta_e^0) \neq 0 \tag{17}$$

$$q_{11}a_{31} - q_{31}a_{11} \neq 0 \tag{18}$$

From Eq. (17), we have the following two cases:

1) $M_w'(\alpha^0)\neq 0$, which implies that $B_t(\alpha^0, \delta_e^0)\neq 0$.

2) $M_w'(\alpha^0)=0$, which implies that $A_w(\alpha^0, \delta_e^0)\neq 0$ and $B_t(\alpha^0, \delta_e^0)\neq 0$.

These two cases can be very easily verified. However, there is no simple form for Eq. (18).

Next, we consider the possibility of the occurrence of Hopf bifurcation. From Eq. (13), we find that Hopf bifurcation may occur if

$$a_{12}a_{31} - (a_{11} + a_{33})(a_{11}a_{33} - a_{13}a_{31}) = 0$$

and

$$(a_{11}a_{33} - a_{13}a_{31}) > 0 \tag{19}$$

Therefore, we obtain a necessary condition for the occurrence of Hopf bifurcation as given hereafter.

Proposition 3: If system (9) has a Hopf bifurcation at $\delta_e=\delta_e^0$, then $a_{12}a_{31}$ and $a_{11}+a_{33}$ have the same sign.

From Propositions 2 and 3, we have the following two corollaries.

Corollary 2: The third eigenvalue of the system (9), except the pair of pure complex eigenvalues at the equilibrium point $\boldsymbol{x}^0$, is stable if 1) $\theta^0<0$ and $a_{31}<0$, or 2) $\theta^0>0$ and $a_{31}>0$.

Corollary 3: The third eigenvalue of the system (9), except the pair of pure complex eigenvalues at the equilibrium point $\boldsymbol{x}^0$, is unstable if 1) $\theta^0<0$ and $a_{31}>0$, or 2) $\theta^0>0$ and $a_{31}<0$.

By the observation from Eq. (19) and the values a_{ij}, we obtain some qualitatively significant results. Because the gravitation constant g is much less than the value of aircraft's speed u, this implies $|a_{12}|\ll 1$. Assuming that a_{31} is not a large number (in general, the assumption is true), we know that the dominant term in Eq. (19) is $(a_{11}+a_{33})(a_{11}a_{33}-a_{13}a_{31})\cong 0$. To determine the possibility of Hopf bifurcation occurring, consider the general case for $0<\alpha^0<\pi/2$. In this situation it is clear that $A_t>0$, but $A_w>0$ before stall while $A_w<0$ in the poststall region because $L_w'(\alpha^0)<0$ after the stall occurs. First, we consider the case of $(a_{11}+a_{33})=0$, which implies $A_w<0$, that is, $L_w'(\alpha^0)<0$. That is, the Hopf bifurcation may occur just after the stall. Next, we consider the condition of $(a_{11}a_{33}-a_{13}a_{31})=0$, which implies that $A_w\gg A_t$. In general, this condition does not hold.

We now check the transversality condition as in Eq. (5) for Hopf bifurcation. Suppose the system (9) possesses Hopf bifurcation at the bifurcation point $\boldsymbol{x}^0$ for $\delta_e=\delta_e^0$. Denote $\lambda_c=\pm iw_c$ as the pair of critical eigenvalues. From Eq. (13), we then have

$$w_c = \sqrt{a_{11}a_{33} - a_{13}a_{31}}$$

Denote $\boldsymbol{l}=[l_1\ \ l_2\ \ l_3]$ and $\boldsymbol{r}=[1\ \ r_2\ \ r_3]^T$, respectively, the right and left eigenvectors of $\boldsymbol{L}_0$ corresponding to the eigenvalue iw_c with $\boldsymbol{lr}=1$. The values of l_i and r_i can then be calculated and are given in Appendix C.

The partial derivative of $\boldsymbol{L}_0$ with respect to δ_e gives

$$\boldsymbol{L}_1 = \frac{\partial}{\partial\delta_e}\boldsymbol{L}_0|_{(\alpha,\delta_e)=(\alpha^0,\delta_e^0)} = \begin{bmatrix}\zeta_{11} & 0 & 0\\ 0 & 0 & 1\\ \zeta_{31} & 0 & 0\end{bmatrix} \tag{20}$$

where the values of ζ_{11} and ζ_{31} are given in Appendix C. Thus, the transversality condition can then be calculated as

$$\Re e\{\boldsymbol{l}\boldsymbol{L}_1\boldsymbol{r}\} = \Re e\{l_1\zeta_{11} + l_3\zeta_{31}\}$$
$$= \frac{1}{2}\zeta_{11}\left(1 - \frac{a_{11}+a_{33}}{a_{31}}\cdot\frac{uml_t}{I_y\cos^2\alpha^0}\right)\neq 0 \tag{21}$$

From Eq. (21), $\zeta_{11}\neq 0$ is a necessary condition for supporting the transversality condition. This implies that

$$A_t^{(0,1)}(\alpha^0, \delta_e^0) = \frac{\partial^2}{\partial\alpha\partial\delta_e}L_t(\alpha, \delta_e)\cos\alpha_t(\alpha, \delta_e)\Big|_{(\alpha,\delta_e)=(\alpha^0,\delta_e^0)} \neq 0 \tag{22}$$

That is, the second derivative of $L_t(\cdot,\cdot)\cos\alpha_t(\cdot,\cdot)$ with respect to α and δ_e at $(\alpha, \delta_e)=(\alpha^0, \delta_e^0)$ is not equal to zero. Equation (22) is simple and not difficult to use in checking the transversality condition at Hopf bifurcation points. It is known that the transitions that emerged from Hopf bifurcation may bring system equilibria to periodic solutions. These imply that the aircraft dynamics may exhibit periodic oscillations.

IV. Numerical Study for F-8 Aircraft

In this section, we first recall the third-order model of longitudinal dynamics for F-8 aircraft.[16] Based on this third-order model, the local stability and bifurcations of flight dynamics are given. The effect of the mass of the aircraft on the existence of equilibrium points is also studied.

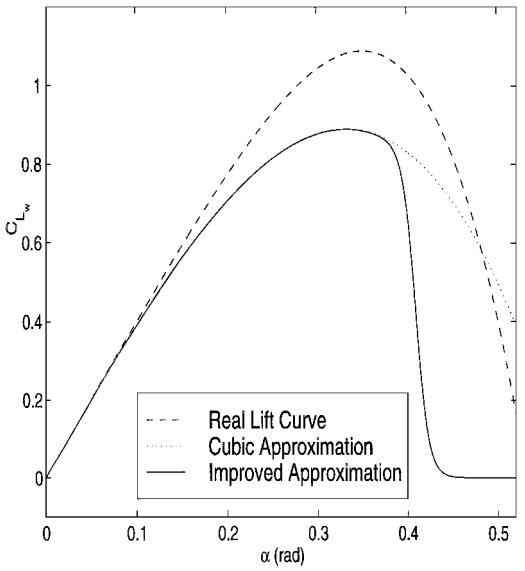

Fig. 1 Lift curve C_{L_w} vs α: real curve, cubic approximation, and improved approximation.

A. Third-Order Model of Longitudinal Dynamics

In 1977, two cubic polynomial functions were proposed to approximate the wing lift and tail lift coefficients as given by[16]

$$L_w = \bar{q}SC_{L_w} = \bar{q}S\left(C^0_{L_w} + C^1_{L_w}\alpha - C^2_{L_w}\alpha^3\right) \tag{23}$$

$$L_t = \bar{q}S_tC_{L_t} = \bar{q}S_t\left(C^0_{L_t} + C^1_{L_t}\alpha_t - C^2_{L_t}\alpha_t^3 + a_e\delta_e\right) \tag{24}$$

where $C^0_{L_w}$, $C^1_{L_w}$, $C^2_{L_w}$, $C^0_{L_t}$, $C^1_{L_t}$, and $C^2_{L_t}$ are constants and depend on the given individual aircraft, δ_e represents the horizontal tail deflection angle measured clockwise from the x axis, and a_e is the linear approximation of the effect of δ_e on C_{L_t}. The relationship between the true wing lift coefficient and the cubic approximation are recalled and depicted in Fig. 1.

Because the horizontal tail of the F-8 is within the wing wake, the downwash angle ϵ has to be included in determining the tail angle of attack. When we use the linear approximation of $\epsilon = a_\epsilon\alpha$, the tail angle of attack is given by

$$\alpha_t = \alpha - \epsilon + \delta_e = (1 - a_\epsilon)\,\alpha + \delta_e \tag{25}$$

As depicted in Fig. 1, the approximation of the wing lift force coefficient proposed by Abed and Lee[12] is more realistic in the stall and poststall regions than the one in Eq. (23). From Ref. 12, the improved wing lift coefficient is recalled and is given here:

$$L_w = \bar{q}S\left(C^0_{L_w} + C^1_{L_w}\alpha - C^2_{L_w}\alpha^3\right)\cdot W \tag{26}$$

where

$$W := \{1/[1 + (\alpha/0.41)^{60}]\}$$

By the use of the aircraft data of Ref. 16 we assume that the aircraft flies at constant velocity of $u = 845.6$ ft/s at an altitude of 30,000 ft. For simplicity and without loss of generality, when we assume the moment of inertia I_y is proportional to m, the equations of motion (8) now become

$$\dot{\alpha} = q\cos^2\alpha + 0.0381\cos^2\alpha\cos\theta - (1/m)(564.434\alpha - 1693.301\alpha^3)\cos^3\alpha\cdot W - (1/m)\left(35.145\alpha - 6.560\alpha^3 + 144.096\delta_e - 79.077\alpha^2\delta_e - 316.309\alpha\delta_e^2 - 421.745\delta_e^3\right) \times \cos^2\alpha\cos(0.25\alpha + \delta_e) \tag{27a}$$

$$\dot{\theta} = q \tag{27b}$$

$$\dot{q} = -(1/m)264.409q + (1/m)(622.222\alpha - 1866.667\alpha^3)\cos\alpha\cdot W - (1/m)\left(3423.386\alpha - 641.885\alpha^3 + 14035.883\delta_e - 7702.619\alpha^2\delta_e - 30810.476\alpha\delta_e^2 - 41080.634\delta_e^3\right) \times \cos(0.25\alpha + \delta_e) \tag{27c}$$

where m denotes the mass of the aircraft.

B. Stability and Bifurcation Analysis

In the following, the analytic results presented in Sec. III is applied to the system (27) by treating δ_e as bifurcation parameter. Choose $m = m_0$, where $m_0 = 667.7$ slugs is adopted from Ref. 16. A computer software package, AUTO, is used to do the numerical analysis because it can calculate the eigenvalues for the Jacobian matrix of every equilibrium point and determine the stability of periodic solutions that emerge from Hopf bifurcation points for the system.

Using AUTO, we find that the system (27) possesses two subcritical Hopf bifurcations HBPO1 and HBPO2 and two saddle-node stationary bifurcations SNBP1 and SNBP2. The locations of these bifurcations are listed in case 1 of Table 1. Figures 2 and 3 show the equilibrium points and periodic solutions that emerge from the bifurcation points for the bifurcation parameter $\delta_e \in [-0.2, 0]$.

From Figs. 2 and 3, we have the following observations:

1) There are no equilibrium points between two limit points, that is, for $\delta_e \in (-0.0999, -0.0090)$. This agrees with Observation 1.

2) The equilibrium states of α and q for $\theta < 0$ are the same as those for $\theta > 0$, but the stability is reversed. This agrees with Observation 2.

3) The occurrence of Hopf bifurcations agrees with Proposition 3.

4) The stability of one of the three eigenvalues for the system (27) depends on the residence of pitch angle θ. These results agree with Corollary 1.

According to the characteristic equation (13) of system (9) and Proposition 2, the stability of system equilibrium depends on the value a_{12} of the Jacobian matrix. For system (27), $a_{12} = -0.03808\cos^2\alpha^0\sin\theta^0$. Because the sine function is an odd function, the value of θ^0, therefore, determines the sign of a_{12} and the stability of one eigenvalue of the system (27). To verify the existence of saddle-node bifurcation, the transversality conditions in Eqs. (17) and (18) are calculated to be satisfied at SNBP1 and SNBP2. From

Table 1 Location of bifurcation points

Label	δ_e, rad	α, rad	θ, rad	q, rad/s
		Case 1, $m = m_0$		
HBPO1	−0.1058	0.4347	1.4588	0.0
HBPO2	−0.1062	0.4360	−1.4773	0.0
SNBP1	−0.0090	0.0448	0.0	0.0
SNBP2	−0.0999	0.4177	0.0	0.0
		Case 2, $m = 5m_0$		
HBPM1	−0.0841	0.3809	0.4817	0.0
HBPM2	−0.1052	0.4326	1.5412	0.0
HBPM3	−0.0827	0.3754	−0.4495	0.0
HBPM4	−0.1070	0.4393	−1.5591	0.0

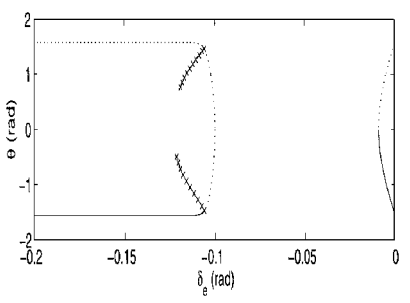

Fig. 2 Equilibria and periodic solutions for the system (27) with $m = m_0$, state θ: ——, stable equilibrium point; ...., unstable equilibrium point; and ×, unstable limit cycle.

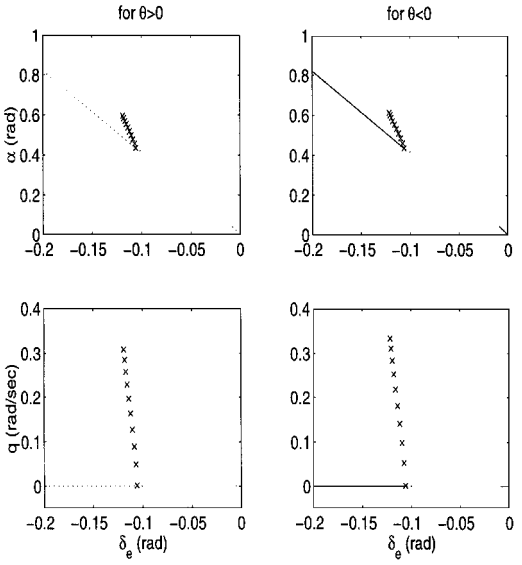

Fig. 3 Equilibria and periodic solutions for the system (27) with $m = m_0$, states α and q.

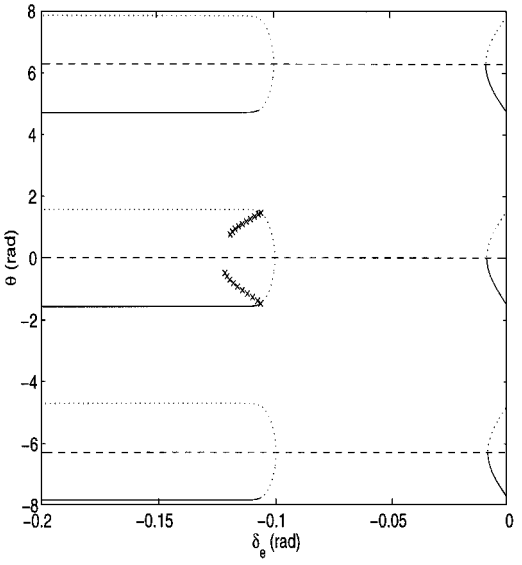

Fig. 4 Repeat of system equilibria in θ for every 2π rad.

Observations 1 and 2 in Sec. III, we know that these are jump transitions at which the system equilibria disappear in a fixed interval $\delta_e \in (-0.0999, -0.0090)$. Because the longitudinal dynamics are only discussed here, it is found that the states are divergent in the discontinuous region of system equilibria. In fact, these are also referred as a stall phenomenon, which implies that the system states exhibit a jump in the flight dynamics of an aircraft as observed in Refs. 1–3, 6, and 12. Figure 4 shows the repeat of system equilibria in θ for every 2π rad, where the occurrence of Hopf bifurcations curves are omitted. Typical time responses for checking the existence of stable equilibrium points of the system (27) are demonstrated for $\delta_e = -0.11$ as shown in Fig. 5.

C. Effect of Aircraft's Mass on Equilibrium Points

From Observation 1 in Sec. III, we know that the mass of aircraft m will affect the existence of equilibrium points. Therefore, we can treat the mass of aircraft m as the second bifurcation parameter. In this section, we discuss the effect of mass m on the existence of system equilibria.

By doing rigorous simulations with different values of m, we find that the two limit points of system (27) become closer to each other as mass m increases and vanishes at the value of $m \cong 4.73 \cdot m_0$, where m_0 is the original value of the mass for an F-8 aircraft.[16] As observed through simulations, not only are the two positions of limit points

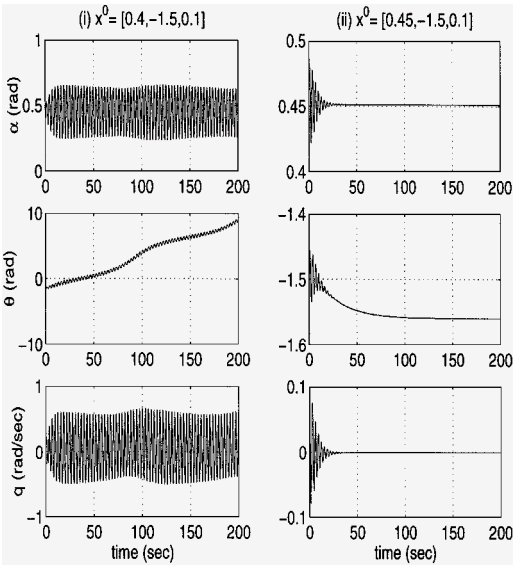

Fig. 5 Time responses for the system (27) with $m = m_0$ at $\delta_e = -0.11$.

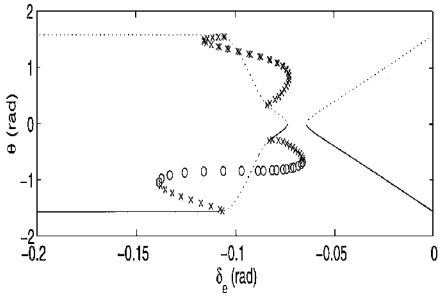

Fig. 6 Equilibria and periodic solutions for the system (27) with $m = 4.7m_0$, state θ: ——, stable equilibrium point; . . . . , unstable equilibrium point; o, stable limit cycle; and ×, unstable limit cycle.

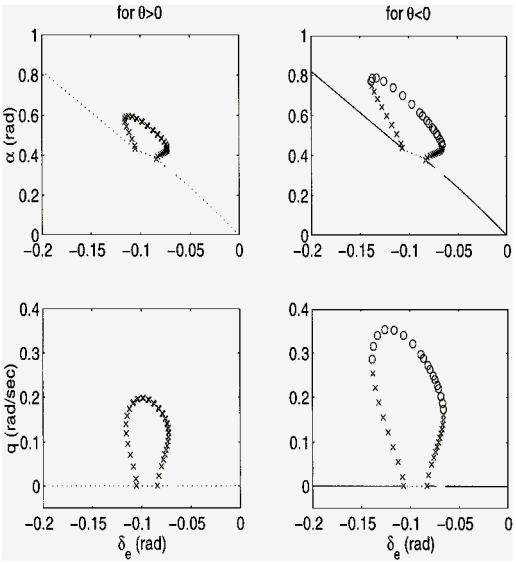

Fig. 7 Equilibria and periodic solutions for the system (27) with $m = 4.7m_0$, states α and q.

moved, but also the bifurcation points are rearranged. Furthermore, when mass is large enough, two new bifurcation points appear, and the periodic solutions emerging from these new bifurcation points meet with each of the original Hopf bifurcations. Figures 6 and 7 show the equilibrium points and periodic solutions for the system (27) with $m = 4.7m_0$. In fact, two cyclic fold bifurcations are also observed for both $\theta > 0$ and $\theta < 0$.

To analyze the qualitative behavior of an aircraft's longitudinal dynamics, the existence and the characteristic of equilibrium points

is very important. Therefore, we modify the original model (27) by increasing the mass m of model (27) to $m = 5m_0$. From simulations in Figs. 8 and 9, these lead to the continuation of system equilibria over the span of all $\delta_e \in [-0.2, 0]$. In addition, we observe that the modified system has two pairs of subcritical Hopf bifurcations. The locations of these four bifurcations are given in case 2 of Table 1. In Figs. 8 and 9, the equilibrium points of the modified system are found to be stable, with the exception of those lying between the two Hopf bifurcation points HBPM3 and HBPM4 for $\theta < 0$, whereas all of the equilibrium points are unstable for $\theta > 0$. Moreover, the periodic solutions that emerge from the pair of Hopf bifurcations HBPM3 and HBPM4 for $\theta < 0$ are observed to be stable limit cycles between two cyclic fold bifurcation points, but the remaining periodic solutions are unstable. Figure 10 shows the time responses for the modified system at $\delta_e = -0.0842$ with initial condition $x^0 = [0.6, -0.86, 0.28]$. These results demonstrate that there exists a stable limit cycle between two cyclic fold bifurcation points for $\theta < 0$. The simulations depicted in Figs. 8–10 agree with those presented in Refs. 1–3, 6, and 12.

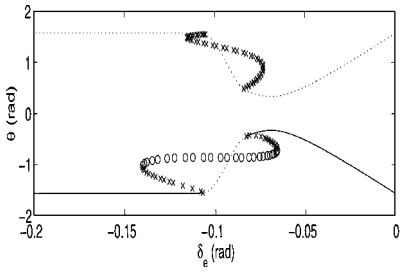

Fig. 8 Equilibria and periodic solutions for the system (27) with $m = 5m_0$, state θ: ——, stable equilibrium point; . . . ., unstable equilibrium point; o, stable limit cycle; and ×, unstable limit cycle.

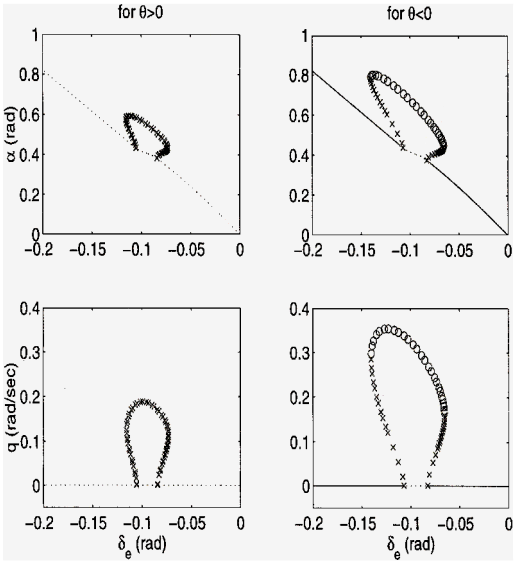

Fig. 9 Equilibria and periodic solutions for the system (27) with $m = 5m_0$, states α and q.

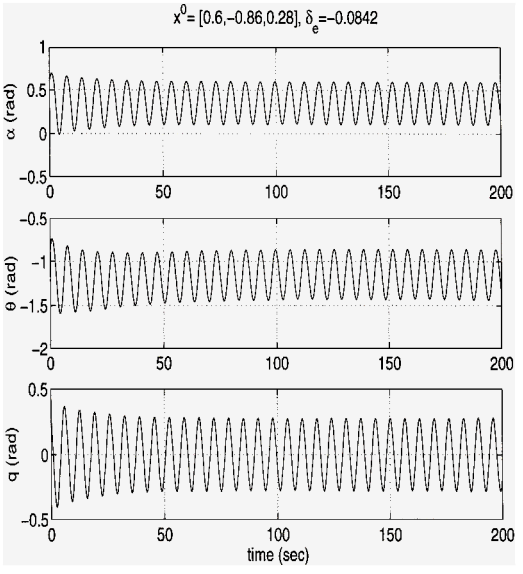

Fig. 10 Time responses for the system (27) with $m = 5m_0$ at $\delta_e = -0.0842$.

V. Conclusions

In this paper, we focused on the study of stability and nonlinear behavior of longitudinal flight dynamics. These are achieved by applying Routh–Hurwitz stability criteria and bifurcation theorems to the third-order model of longitudinal flight dynamics. One of main contributions of this study is that analytic results were obtained for checking the existence of system equilibria and local bifurcations such as Hopf bifurcation and saddle-node bifurcation with respect to the variation of the elevator deflection angle. Numerical results for a typical example of the flight dynamics of F-8 aircraft demonstrate the theoretical analysis. These results agree with the previous observations presented in Refs. 1–3, 6 and 12. In addition, the discontinuity of the system equilibrium, which might contribute to the sudden jump behavior in pitch axis dynamics was observed and was found to disappear as the mass of aircraft increases. This might be a very important issue for the design of fighter aircraft when the mass change becomes significant. From analytical results, Hopf bifurcations were predicted to occur near maximum lift curve only. Numerical simulations also verified such predictions. In this study, we emphasized explaining pitch oscillations and possible instabilities that occur near maximum lift by neglecting the effect of drag. However, the impact of drag on nonlinear longitudinal dynamics might become significant for high-angle-of-attack flight. This issue is very important and might be a good topic for further study.

Appendix A: Values of a_{ij} and b_i

The values of a_{ij} and b_i are given as follows:

$$a_{11} = -\cos^2\alpha^0/(um)\left\{A_w(\alpha^0) + A_t\left(\alpha^0, \delta_e^0\right)\right\}$$

$$a_{12} = -(g/u)\cos^2\alpha^0 \sin\theta^0 \qquad a_{13} = \cos^2\alpha^0$$

$$a_{31} = (1/I_y)\left\{M_w'(\alpha^0) + lA_w(\alpha^0) - l_t A_t\left(\alpha^0, \delta_e^0\right)\right\}$$

$$a_{33} = -c/I_y$$

$$\gamma_1 = \cos^2\alpha^0/(um)\left\{L_t\left(\alpha^0, \delta_e^0\right)\sin\alpha_t\left(\alpha^0, \delta_e^0\right)\alpha_t^{(0,1)}\left(\alpha^0, \delta_e^0\right)\right.$$

$$\left. - L_t^{(0,1)}\left(\alpha^0, \delta_e^0\right)\cos\alpha_t\left(\alpha^0, \delta_e^0\right)\right\} = -\cos^2\alpha^0/(um)B_t\left(\alpha^0, \delta_e^0\right)$$

$$\gamma_3 = (l_t/I_y)\left\{L_t\left(\alpha^0, \delta_e^0\right)\sin\alpha_t\left(\alpha^0, \delta_e^0\right)\alpha_t^{(0,1)}\left(\alpha^0, \delta_e^0\right)\right.$$

$$\left. - L_t^{(0,1)}\left(\alpha^0, \delta_e^0\right)\cos\alpha_t\left(\alpha^0, \delta_e^0\right)\right\} = -(l_t/I_y)B_t\left(\alpha^0, \delta_e^0\right)$$

where u, m, g, c, I_y, l, and l_t are as defined in the Nomenclature.

Appendix B: Values of q_{ij}

The values of q_{ij} are given as follows:

$$q_{11} = -\cos^2\alpha^0/(2um)\left\{\left[A_w'(\alpha^0) + A_t^{(1,0)}\left(\alpha^0, \delta_e^0\right)\right]\cos\alpha^0\right.$$

$$\left. - 4\left[A_w(\alpha^0) + A_t\left(\alpha^0, \delta_e^0\right)\right]\sin\alpha^0\right\}$$

$$q_{12} = -\tfrac{1}{2}ug\cos^2\alpha^0\cos\theta^0$$

$$q_{13} = (2g/u)\cos\alpha^0\sin\alpha^0\sin\theta^0 \qquad q_{14} = -2\cos\alpha^0\sin\alpha^0$$

$$q_{31} = \tfrac{1}{2}I_y\left\{M_w''(\alpha^0) + lA_w'(\alpha^0) - l_t A_t^{(1,0)}\left(\alpha^0, \delta_e^0\right)\right\}$$

where u, m, g, c, I_y, l, and l_t are as defined in the Nomenclature.

Appendix C: Values of l_i, r_i and ζ_{ij}

The values of l_i, r_i and ζ_{ij} are given as follows:

$$l_1 = (iw_c - a_{33})/(2iw_c) \qquad l_2 = a_{12}/(iw_c)l_1$$

$$l_3 = [(iw_c - a_{11})/a_{31}]l_1 \qquad r_2 = a_{31}/[iw_c(iw_c - a_{33})]$$

$$r_3 = a_{31}/(iw_c - a_{33}) \qquad \zeta_{11} = -\cos^2\alpha^0/(mu)A_t^{(0,1)}\left(\alpha^0, \delta_e^0\right)$$

$$\zeta_{31} = -(l_t/I_y)A_t^{(0,1)}\left(\alpha^0, \delta_e^0\right)$$

where u, m, I_y, and l_t are as defined in the Nomenclature and a_{ij} as given in Appendix A.

Acknowledgments

This research was supported by the National Science Council, Taiwan, Republic of China under Grants NSC 84-2212-E009-002 and NSC 89-CS-D-009-013. The authors are grateful to Eyad H. Abed for his helpful discussions during preparation of this work and the reviewers for their comments and suggestions.

References

[1]Carroll, J. V., and Mehra, R. K., "Bifurcation Analysis of Nonlinear Aircraft Dynamics," *Journal of Guidance, Control, and Dynamics*, Vol. 5, No. 5, 1982, pp. 529–536.

[2]Planeaux, J. B., and Barth, T. J., "High Angle-of-Attack Dynamic Behavior of a Model High-Performance Fighter Aircraft," AIAA Paper 88-4368, Aug. 1988.

[3]Planeaux, J. B., Beck, J. A., and Baumann, D. D., "Bifurcation Analysis of a Model Fighter Aircraft with Control Augmentation," AIAA Paper 90-2836, Aug. 1990.

[4]Avanzini, G., and de Matteis, G., "Bifurcation Analysis of a Highly Augmented Aircraft Model," *Journal of Guidance, Control, and Dynamics*, Vol. 20, No. 4, 1997, pp. 754–759.

[5]Gibson, L. P., Nichols, N. K., and Litteboy, D. M., "Bifurcation Analysis of Eigenstructure Assignment Control in a Simple Nonlinear Aircraft Model," *Journal of Guidance, Control, and Dynamics*, Vol. 21, No. 5, 1998, pp. 792–798.

[6]Jahnke, C. C., and Culick, F. E. C., "Application of Bifurcation Theory to the High-Angle-of-Attack Dynamics of the F-14," *Journal of Aircraft*, Vol. 31, No. 1, 1994, pp. 26–34.

[7]Abed, E. H., and Fu, J.-H., "Local Feedback Stabilization and Bifurcation Control, I. Hopf Bifurcation," *System and Control Letters*, Vol. 7, No. 1, 1986, pp. 11–17.

[8]Abed, E. H., and Fu, J.-H., "Local Feedback Stabilization and Bifurcation Control, II. Stationary Bifurcation," *System and Control Letters*, Vol. 8, No. 5, 1987, pp. 467–473.

[9]Guckenheimer, J., and Holmes, P., *Nonlinear Oscillations, Dynamical Systems, and Bifurcations of Vector Fields*, Springer-Verlag, New York, 1983.

[10]Chow, S. N., and Hale, J. K., *Methods of Bifurcation Theory*, Springer-Verlag, New York, 1982.

[11]Howard, L. N., "Nonlinear Oscillation," *Nonlinear Oscillations in Biology*, edited by F. C. Hoppendteadt, American Mathematical Society, Providence, RI, 1979, pp. 1–67.

[12]Abed, E. H., and Lee, H.-C., "Nonlinear Stabilization of High Angle-of-Attack Flight Dynamics Using Bifurcation Control," *Proceedings of the 1990 American Control Conference*, IEEE Publications, Piscataway, NJ, 1990, pp. 2235–2238.

[13]Lee, H.-C., and Abed, E. H., "Washout Filters in the Bifurcation Control of High Alpha Flight Dynamics," *Proceedings of the 1991 American Control Conference*, IEEE Publications, Piscataway, NJ, 1991, pp. 206–211.

[14]Liaw, D.-C., and Abed, E. H., "Stabilization of Tethered Satellites During Station-Keeping," *IEEE Transactions on Automatic Control*, Vol. 35, No. 11, 1990, pp. 1186–1196.

[15]Liaw, D.-C., and Abed, E. H., "Active Control of Compressor Stall Inception: a Bifurcation-Theoretic Approach," *Automatica*, Vol. 32, No. 1, 1996, pp. 109–115.

[16]Garrard, W. L., and Jordan, J. M., "Design of Nonlinear Automatic Flight Control Systems," *Automatica*, Vol. 13, No. 5, 1977, pp. 497–505.